



City Research Online

City, University of London Institutional Repository

Citation: Lamine, D., Djamel, H., Oussama, T., Ayoub, A. & Khechai, A. (2020). Effect of boundary conditions and geometry on the failure of cylindrical shell structures. *Engineering Solid Mechanics*, 8(4), pp. 313-322. doi: 10.5267/j.esm.2020.4.001

This is the published version of the paper.

This version of the publication may differ from the final published version.

Permanent repository link: <https://openaccess.city.ac.uk/id/eprint/25963/>

Link to published version: <https://doi.org/10.5267/j.esm.2020.4.001>

Copyright: City Research Online aims to make research outputs of City, University of London available to a wider audience. Copyright and Moral Rights remain with the author(s) and/or copyright holders. URLs from City Research Online may be freely distributed and linked to.

Reuse: Copies of full items can be used for personal research or study, educational, or not-for-profit purposes without prior permission or charge. Provided that the authors, title and full bibliographic details are credited, a hyperlink and/or URL is given for the original metadata page and the content is not changed in any way.

City Research Online:

<http://openaccess.city.ac.uk/>

publications@city.ac.uk

Effect of boundary conditions and geometry on the failure of cylindrical shell structures**Djouama Mohamed Lamine^{a*}, Hamadi Djamel^a, Temami Oussama^b, Ashraf Ayoub^c and Abdelhak khechai^d**^aLaboratory of Civil Engineering, Hydraulics, Development and Durability, Department of Civil Engineering and Hydraulics, Biskra University, Algeria^bLaboratory of Soil Mechanics and Structures, Mentouri Brothers University, Ain El Bey Street, B.P. 325, 25017 Constantine, Algeria^cSchool of Engineering and Mathematical Sciences, City University London, Northampton Square London EC1V 0HB, United Kingdom^dCivil Engineering Laboratory, University of Biskra, Algeria**ARTICLE INFO***Article history:*

Received 10 January 2020

Accepted 15 April 2020

Available online

15 April 2020

*Keywords:**Cylindrical shell**Experimental tests**Nonlinear analysis**Boundary conditions**Geometrical dimensions**Plastic failure**Strength load***ABSTRACT**

In this paper, experimental and numerical studies are performed to determine the maximum deflection and strength of cylindrical shells. The considered models are subjected to concentrated loads applied progressively until plastic failure of the structures. In order to determine the effect of the geometrical parameters, several models with different thicknesses, lengths, and radius are considered and analysed with various boundary conditions. The numerical analysis is carried out by the finite element method using ABAQUS code. The main objective of the present investigation is to determine the maximum strength that caused damage of the models. The results of the experimental and numerical analysis are recorded, discussed and commented on. It is observed that the thickness, length, and radius dimensions with boundary conditions have great effect on the strength load values that create damage.

© 2020 Growing Science Ltd. All rights reserved.

1. Introduction

Cylindrical shell structures are extensively used in many engineering applications such as tanks, aerospace products and ship construction. During the last few years, structural analysis was made easy through the use of computer software, especially those based on the finite element method. In order to determine the allowable loads of these kinds of structures, it is inevitable to take into account the non-linear material and/or geometrical behaviour in the analysis for best design purpose. However, due to the importance of the non-linear analysis of shells, numerous researchers have attempted to develop finite elements that can provide efficient results. Parisch (1981) proposed a mathematical formulation of shell elements with large deflections to predict the elasto-plastic material behaviour. The elements utilized are the so-called degenerated shell elements, with special emphasis on the simple quadrilateral element with four nodes. Huang (1989) adopted a strain element to investigate the elastic and elasto-plastic behaviour of shells with isotropic and anisotropic materials. In the element formulation, he used shear and membrane strain fields to overcome the locking problem. Argyris et al. (2002) added an elastoplastic constitutive model based on the von-Mises yield criterion with isotropic hardening. This criterion is incorporated into the triangular element. Skopinsky et al. (2015) defined the plastic limit load in shell

* Corresponding author.

E-mail addresses: m.djouama@univ-biskra.dz (D. M. Lamine)

intersections under combined loading using nonlinear finite element analysis. They described an application of nonlinear analysis for investigation of the elastic-plastic behaviour. In the same year, Beheshti and Ramezani (2015) developed an efficient finite element formulation to analyze large elastic deformations of functionally graded (FG) shell structures. In this formulation, all strain and stress components are accurately determined. Jeon et al. (2015) presented the MITC3 + shell finite element for geometric nonlinear analysis and demonstrated its performance. They used the total Lagrangian formulation with large displacements and large rotations. Caseiro et al. (2015) revised and extended assumed natural strain for a quadratic NURBS-based solid-shell element for the analysis of large deformation elasto-plastic thin shell structures. Rajabiehfarid et al. (2016) studied the dynamic buckling of axisymmetric circular cylindrical shells subjected to an axial impact theoretically and experimentally. The von Mises yield criterion is used for the elastic-plastic cylindrical shell made of linear strain hardening material in order to derive the constitutive relations between the stress and strain increments, the nonlinear equations are solved with the finite difference method for two types of loadings which are stationary cylindrical shells impacted axially, and traveling cylindrical shells impacted against a rigid wall. The experimental tests for the two types of loadings are performed by Gas gun. Chen et al. (2016) studied the plastic collapse mechanisms of uniaxially-loaded cylindrical shell-plate periodic honeycombs with identical mass (or relative density) but varying geometric parameters, by series of in-plane and out-of-plane experiments and finite element numerical simulations, and they developed a concept to optimize lattice structures by combining different substructures. Burzyński et al. (2016) assumed the formulation of the elastic constitutive law for functionally graded materials (FGM) on the grounds of nonlinear parameter shell theory with the sixth parameter being the drilling degree of freedom. The material law is derived by through-the-thickness integration of the Cosserat plane stress equations. The constitutive equations are formulated with respect to the neutral physical surface. The influence of the power-law exponent, micro polar characteristic length is evaluated in geometrically nonlinear finite element method (FEM) analyses. The results obtained with the neutral physical surface approach are compared with those computed with the middle surface approach. Borković et al. (2017) conducted a geometric nonlinear static analysis of prismatic shells using the semi-analytical finite strip method. The new computational model, which includes a fully nonlinear compound strip with a longitudinal and transverse stiffener, has been presented. Furthermore, strips with non-uniform characteristics in the longitudinal direction have been used in the nonlinear analysis. Also, the author described the design and implementation of eighteen ideal boundary conditions using three different longitudinal and six well-known transverse displacement interpolation functions. The results of the presented study were obtained using an open-source software and multi-purpose software ABAQUS. Moreover, the accuracy of the applied computational approach has been verified by comparison with results from the literature. Wu et al. (2018) carried out an experimental investigation on Q235 steel cylindrical shell-water-cylindrical shell (*CWC*) structures subjected to near-field or contact underwater explosion loading. All tests were conducted in an artificial water pool detonating 50 g charge weight of trinitrotoluene (TNT) explosive. The corresponding plastic deformation of the *CWC* structures was measured for different structural parameters and standoff distances. Three major deformation modes including seven typical subdivided deformation characteristics were classified and analyzed considering the effect of standoff distance, shell thickness, and water interlayer thickness.

In the investigations performed so far, it is observed that the nonlinear behavior of cylindrical shells subjected to a concentrated load at the middle of the structure is not well studied. On the other hand, the nonlinear behavior of these structures is necessary for the structural design purpose. In this study, different geometric and material parameters are used to test their effect on the cylindrical shell behavior for the models used. The numerical analysis is performed by using the finite element software “ABAQUS” in order to determine the failure load that creates damage of cylindrical shells. To validate the obtained numerical results, experimental investigations are also carried out.

2. Experimental investigation

The experimental investigations presented here have been conducted at the Civil Engineering Laboratory at City, University of London (UK). The important steps of the test's procedures are explained in the next sections.

2.1 Experimental setup

The present study was performed on two cylindrical shell models; each model made of stainless steel 304 and with different thicknesses, but with the same shape and dimensions. The shape is a semi-cylinder with $R = 160$ mm of the radius and $L = 900$ mm length (Fig. 1). The first test is conducted on a cylindrical shell with no end diaphragms and the thickness is $t = 2$ mm (i.e. case CSND2). In this test, several loads are applied and the vertical displacement at the top middle of the model is recorded. The second test is performed similar to the previous model, but the thickness of the shell is $t = 1.2$ mm (i.e. case CSND12). The positioning of the specimen on the UNIFLEX 300 machine is shown in Fig. 2. The loads are applied under displacement-control and the vertical displacements in the middle of the top models are recorded.



Fig. 1. The cylindrical shell model

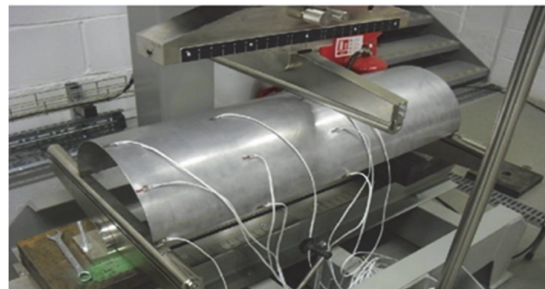


Fig. 2. The specimen on UNIFLEX 300 machine

2.2. Mechanical properties of the used models

In the present experimental study, all the specimens have the same material properties. The specimens were manufactured from a commercially available Stainless steel 304 with an elasticity modulus $E = 190000$ MPa and Poisson's ratio $\nu = 0.265$. In order to simulate numerically the non-linear behaviour of the used material and determine the strength of these cylindrical shells, one needs to use the non-linear data obtained experimentally from a tensile test. The non-linear stress-strain values obtained from the tensile test for stainless steel 304 are presented in Fig. 3.

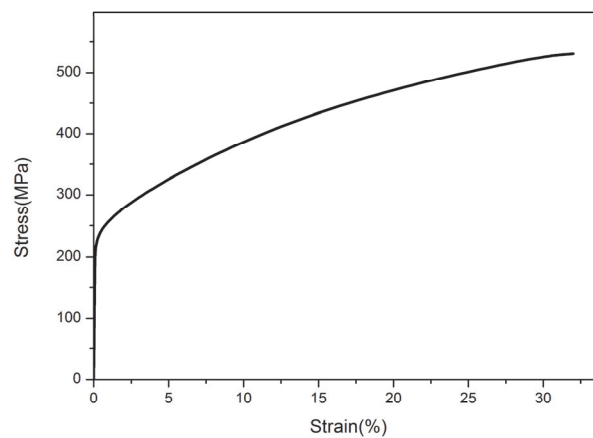


Fig. 3. Stress-strain values of stainless steel 304 obtained from a tensile test

3. Description of the numerical analysis

The models used in the experimental tests have been simulated numerically using the maximum values of applied loads obtained experimentally. The main aim of the experimental investigation is to validate the numerical models by comparing the numerical values of the deflections and strength with those obtained experimentally. Two examples have been chosen to validate the numerical models (two pinned cylindrical shells with thickness values of 1.2 and 2 mm, respectively). The numerical analysis is performed using the finite element method with ABAQUS software version 6.14 (2014), with consideration of the nonlinear behavior. The 3D-shell extrusion is utilized. The cylindrical models are subjected to concentrated loads in the top middle of the shell and both deflections and strength are calculated. The S4R quadrilateral finite-membrane-strain element with a uniformly reduced integration to avoid shear and membrane locking is used. These cylindrical shells are modeled with a regular mesh 10×10 (Temami et al. 2017). The geometric and material properties used in the numerical study are the same as for the experimental tests. The solution adopted to solve the nonlinear problems is the full Newton-Raphson method and the default automatic load incrementation scheme in ABAQUS code. The maximum applied load is automatically subdivided into load increments that are not necessarily uniform. The results obtained from the experimental investigation for both models under consideration are summarized in Table 1 and Figs. 4 and 5. The load- displacement curves obtained from the numerical and experimental investigation for both models are presented in Figs. (4- 5). Fig. 4 shows the load-displacement curve obtained from the experimental and numerical study for the first test model -Pinned Cylindrical Shell Model under the progressive applied load up to load 8386 N (CSND, $t = 2$ mm).

Table.1. Maximum displacement values of Pinned Cylindrical Shell Models (CSND2, $t = 2$ mm and $P=8386$ N)

Test Model	Experimental test (mm)	Numerical analysis (mm)
(CSND2), ($t=2$ mm, $P=8386$ N)	34.26	38.70
(CSND12), ($t=1.2$ mm, $P=3365$ N)	40.11	41.28

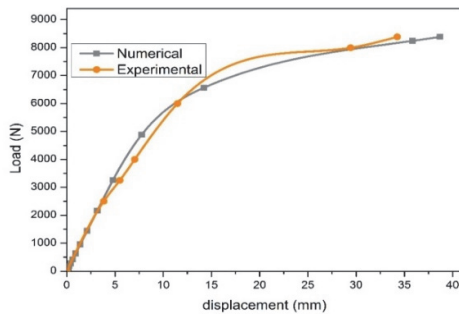


Fig. 4. Numerical and Experimental load-displacement curves of Pinned Cylindrical Shell Model (CSND2, $t = 2$ mm and $P = 8386$ N)

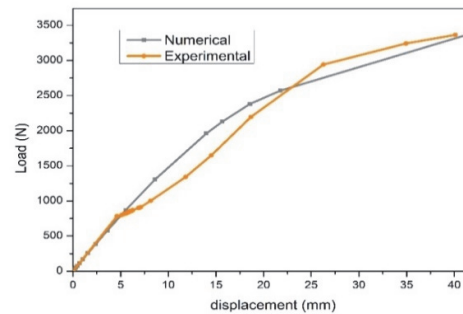


Fig. 5. Numerical and Experimental Force-Displacement Pinned Cylindrical Shell Model (CSND12, $t = 1.2$ mm, $P = 3365$ N)

The following comments can be drawn:

- It can be seen from Fig. 4 that both curves have identical behavior and the curves almost overlap each other.
- There are three distinct regions in the behavior of this model; the first one is the initial elastic region where the behavior is essentially linear up to approximately 2500 N. Here, both experimental and numerical curves overlap each other.

- Following this region, the curves lose relatively their linearity and start to plastify, and the third region follows a nonlinear behaviour with the increases of load starting from 6000 N until final rupture.

Similar comments can be drawn for the second cylindrical shell model with thickness $t = 1.2$ mm (CSND12, $P=3365$ N; shown in Fig. 5). It can be observed from the figure that the numerical model can give a very good response to the analysed specimens in comparison to the experimental test. The difference observed with the experimental curve might be due to the parasites occurred during the application of the increased loading.

4. Parametric study

After validating the accuracy and efficiency of the numerical model against the experimental results, we present in this section a parametric study which aims to determine the effect of the geometrical parameters of the cylindrical shell, i.e. the thickness, the length, and the radius, on the strength/load of the cylindrical shell models in one hand; and in the other hand, to evaluate the effect of the support boundary conditions considered. For this, the following shell models and boundary conditions cases are considered as presented in (Fig. 6):

- Semi cylinder shell model pinned on four corner points (4PP)
- Semi cylinder shell model clamped on four corner points (4CP)
- Semi cylinder shell model pinned on four sides (4PS)
- Semi cylinder shell model clamped on four sides (4CS)

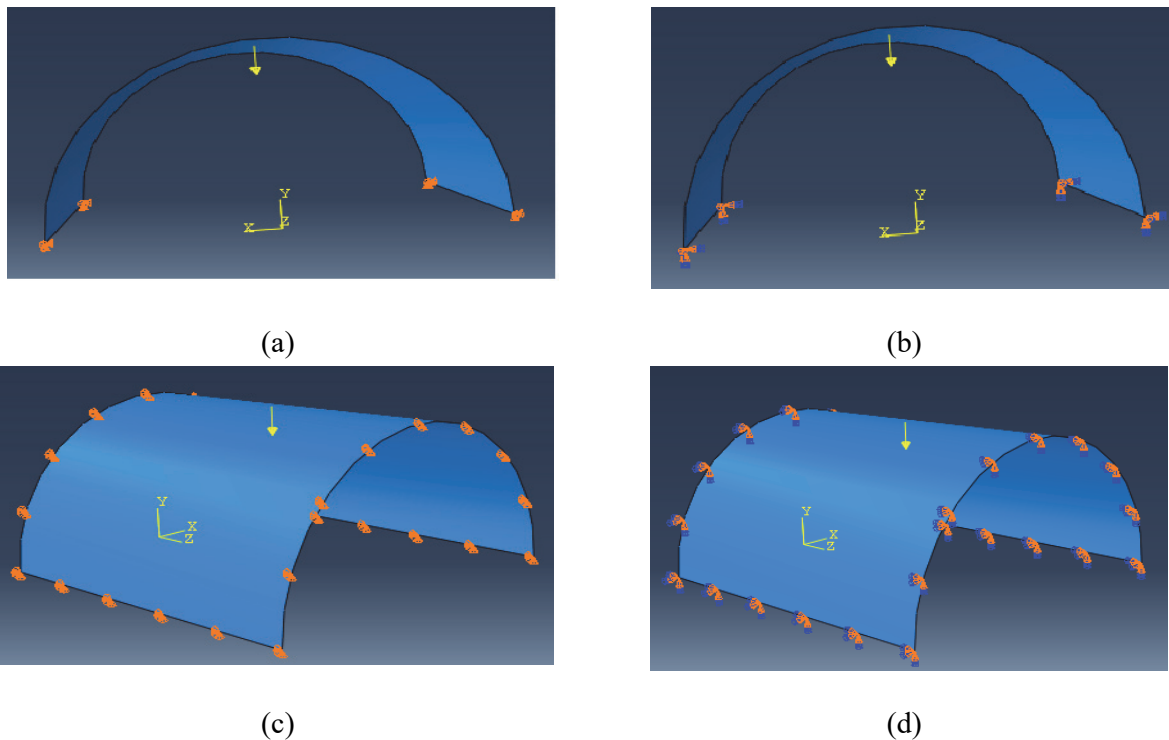


Fig. 6. Cylindrical shell model supported on different boundary conditions: (a) Pinned on four corner points (4PP), (b) Clamped on four corner points (4CP), (c) Pinned on four sides (4PS), (d) Clamped on four sides (4CS)

4.1 The effect of the cylinder thickness

For the first example, a cylinder shell with a circular radius of $R = 160$ mm and length $L = 900$ mm with different thickness values and boundary conditions have been analysed. The thickness values are ranging from 1 mm to 3 mm with 0.2 mm increment. As it mentioned before, the aim of the present investigation is to determine the strength load that can be supported using different thickness and

boundary conditions. The maximum strength load obtained are presented in Table 2 and plotted in Fig. 7. From Table 2 and Fig. 7, it is observed that the value of the optimum strength load is increased with the increase of the thickness values. In addition, the clamped boundary conditions provide more strength values compared to the pinned one. This is most likely related to the additional stiffness given by the clamped support in comparison to the pinned support. Also, a significant increase of the strength load can be obtained with clamped and pinned supports on four sides.

Table. 2. Maximum strength load of cylindrical shell models with different boundary conditions and thicknesses

Thickness (mm)	Strength load (KN)			
	Pinned Cylinder (4PP)	Clamped Cylinder (4CP)	Pinned Cylinder (4PS)	Clamped Cylinder (4CS)
1	9.3363	12.923	115.272	139.408
1.2	13.491	18.616	168.352	186.03
1.4	18.362	25.339	209.941	236.923
1.6	23.984	33.096	267.353	299.524
1.8	30.355	41.888	333.715	370.974
2	37.475	51.714	375.78	431.909
2.2	45.345	62.574	439.616	512.483
2.4	53.964	74.468	518.769	591.288
2.6	63.333	87.396	576.268	669.469
2.8	73.452	101.359	648.004	753.939
3	84.32	116.355	731.385	848.426

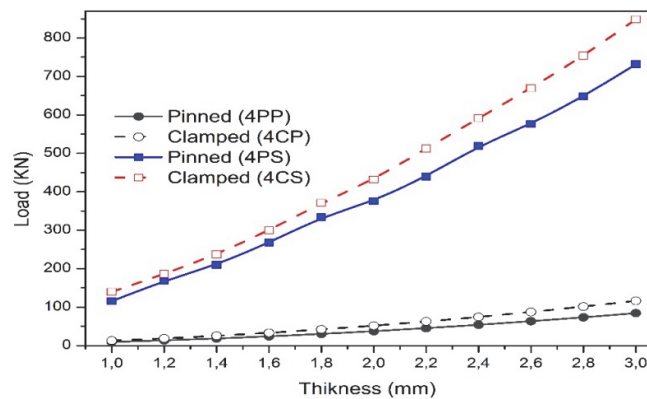


Fig. 7. Strength load of cylindrical shell models with different boundary conditions and thickness values.

4.2 The effect of the cylinder length

In addition to the cases considered in the previous examples, semi-cylinders with a circular radius of $R = 1.5$ m and thickness $t = 5$ mm with different length values and boundary conditions are analysed. The aim of the present investigation also is to determine the strength load that can be supported using different length values and various boundary conditions. The maximum strength loads obtained are presented in Table 3 and plotted Fig. 8. From the values of the maximum strength load obtained with the numerical analysis presented in Table 3 and plotted in Fig.8, the maximum strength is decreased by increasing the length of the model for the case of pinned and clamped supports on four sides (pinned 4PS and clamped 4CS). The situation is vice-versa for pinned and clamped on four supports (pinned 4PP

and clamped 4CP), i.e increase in the ultimate load by increasing the length of the cylinder shells. This can be explained that pinned or clamped supports only on four points allow more deflections with late occurring failure; contrarily to the pinned and clamped model on four sides; and mathematically there is a decrease of the stiffness parameters with the higher deformed shapes that it can be seen from (Fig. 9a and b).

Table 3. Strength load of cylindrical shell models with different length values and various boundary conditions.

Length (m)	Strength load (KN)			
	Pinned Cylinder (4PP)	Clamped Cylinder (4CP)	Pinned Cylinder (4PS)	Clamped Cylinder (4CS)
3	83.79	114.922	4212.264	4898.254
5	138.798	191.535	3527.404	3968.554
7	208.194	287.303	3458.484	3764.754
9	249.831	344.764	3426.154	3753.024

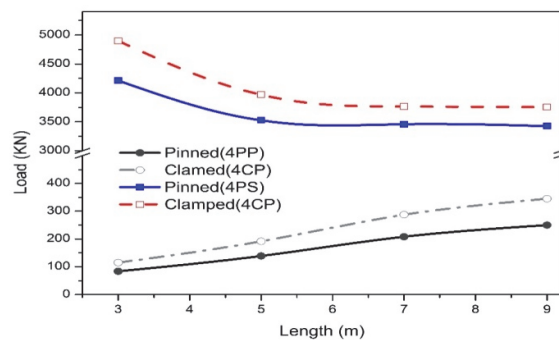
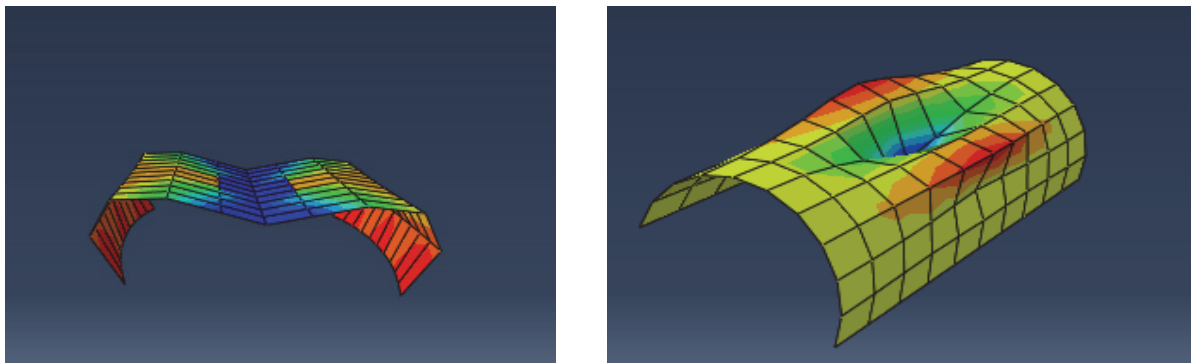


Fig. 8. Strength loads of cylindrical shell models with different length values and various boundary conditions.



(a)

(b)

Fig. 9. Deformed shape of the Cylindrical shell, (a) Pinned on four corner points (4PP), (b) Clamped on four sides (4CS)

4.3. The effect of the cylinder radius

In this section, semi-cylinder models with a length of $L=9$ m and thickness of $t=5$ mm with different radius values and boundary conditions have been studied. The radius values are ranging from 1.5 mm to 4.5 mm with 2 mm increment. The ultimate loads obtained numerically are recorded in Table 4 and plotted in Fig. 10. From the values of the maximum strength load obtained and presented in Table 4 and plotted in Fig. 10, the maximum strength is decreased by increasing the radius of the model for the case

of pinned and clamped on four sides (pinned 4PS and clamped 4CS). The situation is vice-versa for pinned and clamped supports on four points (pinned 4PP and clamped 4CP). In addition, the clamped cylinder can support higher loading compared to the simply supported or clamped on four points only. The increase of strength load in the case where the pinned and clamped on four sides supports (pinned 4PS and clamped 4CS), provide more resistance to the shell, as it can be seen from (Fig.11 a and b).

Table 4. Strength loads of cylindrical shell models with different radius and various boundary conditions

Radius (m)	Strength load (KN)			
	Pinned Cylinder (4PP)	Clamped Cylinder (4CP)	Pinned Cylinder (4PS)	Clamped Cylinder (4CS)
1.5	249.831	344.764	3426.154	3753.024
2.5	149.903	206.86	3946.264	4137.914
3.5	107.073	147.757	4300.534	4499.284
4.5	83.279	114.922	4517.204	4791.514

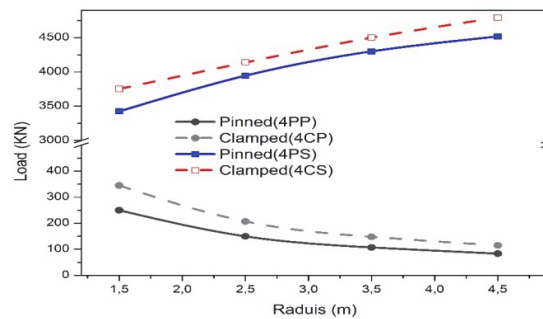


Fig.10. Strength loads of cylindrical shell models with various radius values and different boundary conditions

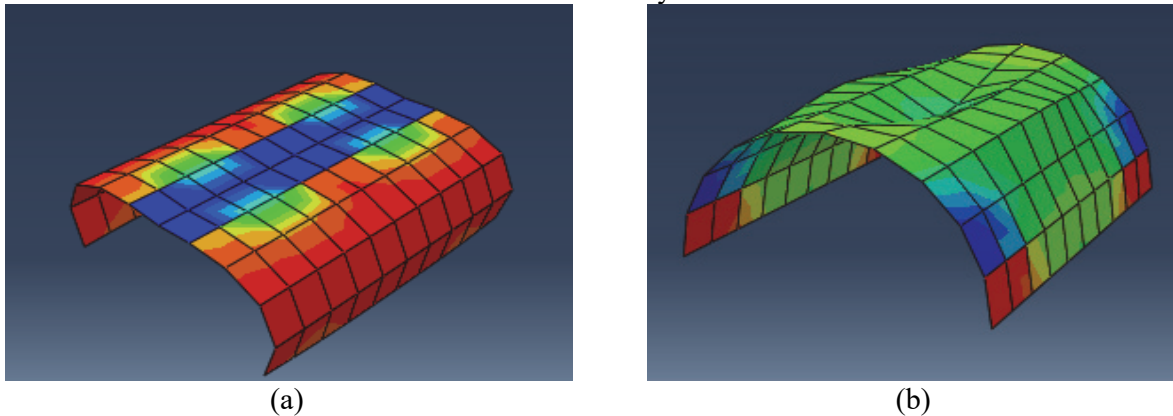


Fig. 11. Deformed shape of the Cylindrical Shell, (a)Pinned on four corner points (4PP), (b) Clamped on four sides (4CS)

5. Conclusion

In this paper, we present the effect of the thickness, length, radius and boundary conditions on the nonlinear behavior and failure of cylindrical shells structures. The models are subjected to concentrated loads at the center of the top surface. Also, the nonlinear behavior of these structures is studied and compared to the experimental results. The aim of this investigation is to help researchers and designers to choose the appropriate model for their needs. According to the results obtained, the effect of thickness is very important, a small difference in the amount of thicknesses (0.2 mm) can increase the strength load of the shell by more than 23%. In addition, the increase of the length values in the case where the boundary conditions are pinned or clamped on four sides decrease the strength load; but for four pinned

or clamped point supports, there is an increase in the strength. This does not prevent that the first case can withstand a load greater than the second one more than 3000 kN. Also, the increase of the radius in the case where the boundary conditions are pinned or clamped on four sides increase the amount of the strength load, but for four pinned or clamped point supports, it decreases the strength load. From the study, it is clear that the influence of the boundary conditions, thickness, length, and radius are very significant.

Acknowledgments

The authors would like to thank all people involved in this work at the Structural Engineering laboratory of City, University of London. Special thanks are due to Dr. Brett McKinley, the laboratory manager for his invaluable advices regarding the test rig setup, Mr. JN Hooker the laboratory technician for the preparation of models, as well as Mr. S Gendy, Mr. R. Mohammad, and Mr. D Das for their help to construct the models.

References

- ABAQUS.(2014). Version 6.14, D. S. S. C.
- Argyris, J. H., Papadrakakis, M., & Karapitta, L. (2002). Elasto-plastic analysis of shells with the triangular element TRIC. *Computer Methods in Applied Mechanics and Engineering*, 191(33), 3613-3636.
- Beheshti, A., & Ramezani, S. (2015). Nonlinear finite element analysis of functionally graded structures by enhanced assumed strain shell elements. *Applied Mathematical Modelling*, 39(13), 3690-3703.
- Borković, A., Kovačević, S., Milašinović, D. D., Radenković, G., Mijatović, O., & Golubović-Bugarški, V. (2017). Geometric nonlinear analysis of prismatic shells using the semi-analytical finite strip method. *Thin-Walled Structures*, 117, 63-88.
- Burzyński, S., Chróścielewski, J., Daszkiewicz, K., & Witkowski, W. (2016). Geometrically nonlinear FEM analysis of FGM shells based on neutral physical surface approach in 6-parameter shell theory. *Composites Part B: Engineering*, 107, 203-213.
- Caseiro, J. F., Valente, R. A. F., Reali, A., Kiendl, J., Auricchio, F., & de Sousa, R. A. (2015). Assumed natural strain NURBS-based solid-shell element for the analysis of large deformation elasto-plastic thin-shell structures. *Computer Methods in Applied Mechanics and Engineering*, 284, 861-880.
- Chen, Q., Shi, Q., Signetti, S., Sun, F., Li, Z., Zhu, F., ... & Pugno, N. M. (2016). Plastic collapse of cylindrical shell-plate periodic honeycombs under uniaxial compression: experimental and numerical analyses. *International Journal of Mechanical Sciences*, 111, 125-133.
- Huang, H. C. (1989). Elastic and elasto-plastic analysis of shell structures using the assumed strain elements. *Computers & Structures*, 33(2), 327-335.
- Jeon, H. M., Lee, Y., Lee, P. S., & Bathe, K. J. (2015). The MITC3+ shell element in geometric nonlinear analysis. *Computers & Structures*, 146, 91-104.
- Temami, O., Hamadi, D. & Bennoui, I. (2017). Numerical and experimental investigation of the behaviour of cylindrical shells. *Asian Journal of Civil Engineering*, 18(8), 1195-1210.
- Parisch, H. (1981). Large displacements of shells including material nonlinearities. *Computer Methods in Applied Mechanics and Engineering*, 27(2), 183-214.
- Rajabiehfarid, R., Darvizeh, A., Darvizeh, M., Ansari, R., Alitavoli, M., & Sadeghi, H. (2016). Theoretical and experimental analysis of elastic-plastic cylindrical shells under two types of axial impacts. *Thin-Walled Structures*, 107, 315-326.
- Skopinsky, V. N., Berkov, N. A., & Vogov, R. A. (2015). Plastic limit loads for cylindrical shell intersections under combined loading. *International Journal of Pressure Vessels and Piping*, 126, 8-16.
- Wu, J., Long, Y., Zhou, Y., Yu, Y., & Liu, J. (2018). Experimental study on the deformation and damage of cylindrical shell-water-cylindrical shell structures subjected to underwater explosion. *Thin-Walled Structures*, 127, 654-665.



© 2020 by the authors; licensee Growing Science, Canada. This is an open access article distributed under the terms and conditions of the Creative Commons Attribution (CC-BY) license (<http://creativecommons.org/licenses/by/4.0/>).